

A Minimalist Optimizer Design for LLM Pretraining

Athanasios Glentis ^{*} Jiaxiang Li [†] Andi Han [‡] Mingyi Hong [§]

Abstract

Training large language models (LLMs) typically relies on adaptive optimizers such as Adam, which require significant memory to maintain first- and second-moment matrices, which are known as *optimizer states*. While recent works such as GaLore, Fira and APOLLO have proposed state-compressed variants to reduce memory consumption, a fundamental question remains: What is the *minimal* amount of optimizer state that is truly necessary to retain state-of-the-art performance in LLM pretraining? In this work, we systematically investigate this question using a bottom-up approach. We find that two (memory- and compute-efficient) optimization techniques are particularly effective: (1) column-wise gradient normalization significantly boosts the performance of plain SGD without requiring momentum; and (2) adding first-order momentum only to the output layer – where gradient variance is highest – yields performance competitive with fully adaptive methods such as Muon. Based on these insights, we propose SCALE (Stochastic Column-normAlized Last-layer momEntum), a new optimizer that combines column-normalized SGD with last-layer momentum, where column normalization refers to normalizing the gradient along the output dimension. Across multiple LLaMA models (60M–1B), SCALE matches or exceeds the performance of Adam while using only 35–45% of the total memory. It also consistently outperforms memory-efficient optimizers such as GaLore, Fira and APOLLO, making it a strong candidate for large-scale pretraining under memory constraints. For LLaMA 7B model, SCALE outperforms the state-of-the-art method APOLLO, in terms of both perplexity and memory consumption. In addition, our method serves as a minimalist baseline for a more sophisticated optimizer design. Code is available at this [link](#).

1 Introduction

Adaptive optimizers such as RMSProp (Hinton et al., 2012), Adam (Kingma and Ba, 2015) are the default optimizers for large-scale attention-based deep neural networks, particularly large language models (LLMs). While effective, these optimizers incur significant memory overhead due to their reliance on maintaining both first- and second-moment estimates of the gradient, which are also known as *optimizer states*. For example, Adam requires storing two additional tensors per parameter tensor, tripling the memory usage compared to vanilla stochastic gradient descent (SGD).

On the other hand, despite its superior memory efficiency, the vanilla SGD performs poorly when applied directly in LLM training, due to the absence of adaptive scaling in the update step (See Figure 2 for experiment results, also see Zhao et al. (2025); Zhang et al. (2020b)). This has motivated a wave of recent research focused on developing memory-efficient alternatives to Adam that aim

^{*}Department of Electrical and Computer Engineering, University of Minnesota. Equal contribution. glent007@umn.edu

[†]Department of Electrical and Computer Engineering, University of Minnesota. Equal contribution. li003755@umn.edu

[‡]School of Mathematics and Statistics, University of Sydney. RIKEN AIP. andi.han@sydney.edu.au

[§]Department of Electrical and Computer Engineering, University of Minnesota. mhong@umn.edu

to retain its performance while reducing memory consumption. These include compression-based algorithms such as GaLore (Zhao et al., 2024) and Adam-Mini (Zhang et al., 2024), as well as novel designs such as Muon (Jordan et al., 2024), Sophia (Liu et al., 2024), SGD-SaI (Xu et al., 2024), Scion Pethick et al. (2025) and SWAN (Ma et al., 2024). These approaches often introduce new algorithmic components—such as different forms of gradient normalization, momentum variants, or second-order approximations—and combine them in various ways.

However, despite the growing literature on memory-efficient optimizers, there has been no systematic study to identify which specific algorithmic components or techniques are most essential for designing highly-performed yet minimal-memory optimizers. For instance, are both first- and second-order momentum terms strictly necessary for effective training? Among the many forms of gradient normalization, which subset of them strike the best trade-off between performance, memory, and computational cost? In the absence of such a principled investigation, it remains unclear how to balance optimizer complexity against memory savings.

This motivates our central research question:

What is the minimum subset of optimizer states beyond the SGD that is required to achieve state-of-the-art pretraining performance?

In this work, we pursue this question through a bottom-up, minimalist approach. Rather than combining a large number of techniques, we systematically evaluate the contributions of basic components – such as normalization and momentum – to identify the minimal set of techniques (on top of vanilla SGD) that are necessary to match Adam-level performance. Concretely, we:

- (1) Identify two key components that can effectively enhance the performance of vanilla SGD: gradient normalization and first-order momentum;
- (2) Analyze how these components can be adapted in the most memory- and compute-efficient manners;
- (3) Justify our design choices using a combination of theoretical insights and empirical evidence.

Our study suggests that two techniques, when used together, are particularly effective: (i) column-wise gradient normalization, which improves SGD performance significantly without requiring momentum; and (ii) adding first-order momentum exclusively to the output layer, where gradient variance is highest (see Figure 3). These insights lead us to propose Stochastic Column-normalized Last-layer momentum (SCALE), a minimalist optimizer that combines these two techniques, which requires roughly the same amount of memory as compared to vanilla SGD. For example, for 1B (resp. 7B) model, SCALE only requires 10% (resp. 2%) more memory as compared to vanilla SGD. Meanwhile, SCALE achieves competitive performance as compared with SOTA optimizers Adam and Muon, with only 35% and 52% of the memory cost for training 1B models, respectively. See Figure 1 for an illustration of performance and memory trade-off among different SOTA algorithms.

1.1 Related Works

Memory-efficient variations of Adam. A recent line of works aims to improve memory efficiency of Adam, compressing the historical states stored, namely the first- and second-order statistics by the use of gradient projections. GaLore (Zhao et al., 2024), being one of the pioneering works, stores the states in a low-rank subspaces that captures most gradient information. Fira (Chen et al., 2024) achieves superior performance than GaLore by re-introducing full-rank information to the low-rank gradients. APOLLO (Zhu et al., 2024) constructs the update based on gradient scaling factors that are estimated from the ratio between the low-dimensional gradient and the low-dimensional Adam update; APOLLO-Mini is a memory efficient version of APOLLO by estimating in a rank-1 subspace.

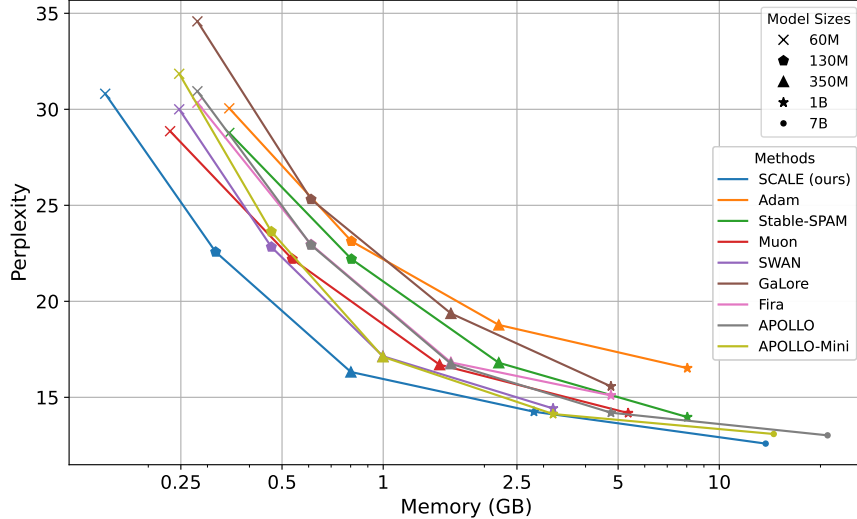


Figure 1: Perplexity v.s. memory consumption among a number of SOTA algorithms. Solutions achieved towards the left-bottom side of the plot represent better performance/memory trade-off (see Appendix A.1 for the details of the memory estimation).

GRASS (Muhammed et al., 2024) improves GaLore by designing sparse projection matrices guided by the norm of the rows of the gradients. SlimAdam (Kalra et al., 2025) compresses second-order moments based on signal-to-noise analysis. Some other methods group parameters into blocks and apply block-wise updates (Luo et al., 2024; Ramesh et al., 2024; Pan et al., 2024), block-wise scaling (Zhang et al., 2024), channel-wise scaling (Zhu et al., 2025), to further reduce the memory costs.

Towards stateless optimizers. More recent works start to question the necessity of optimizer states as required by Adam. Adafactor (Shazeer and Stern, 2018) is perhaps the first work to record the momentum of the column and row norms of the gradient matrix, reducing the memory of optimizer states from $\mathcal{O}(d^2)$ to $\mathcal{O}(d)$ (assuming that the gradient matrix is d by d). SWAN (Ma et al., 2024) combines two gradient normalizations (singular-value and row-wise normalizations, see Section 2), which matches the performance of Adam (when applied only to the intermediate layers while the first and last layers still use Adam. See Section 4 for details). Zhao et al. (2025) demonstrates SGD with signed momentum is able to recover the performance of Adam. SGD-SaI (Xu et al., 2024) verifies that proper learning-rate scaling at initialization is sufficient to achieve good performance.

Novel optimizers with better performance than Adam. Another line of work focuses on proposing new optimizers to achieve improved convergence properties compared to Adam. SPAM and Stable-SPAM (Huang et al., 2025b,a) reset momentum and clip spike gradients, stabilizing mixed-precision LLM training and yield better performance than Adam. Sophia (Liu et al., 2024) accelerates training by leveraging an estimated diagonal Hessian. Muon (Jordan et al., 2024) proposes gradient orthogonalization to further stabilize and enhance LLM training. Other approaches (Bernstein and Newhouse, 2024; Pethick et al., 2025; Kalra et al., 2025) explore various (layer-wise) normalization schemes to design better adaptive optimizers.

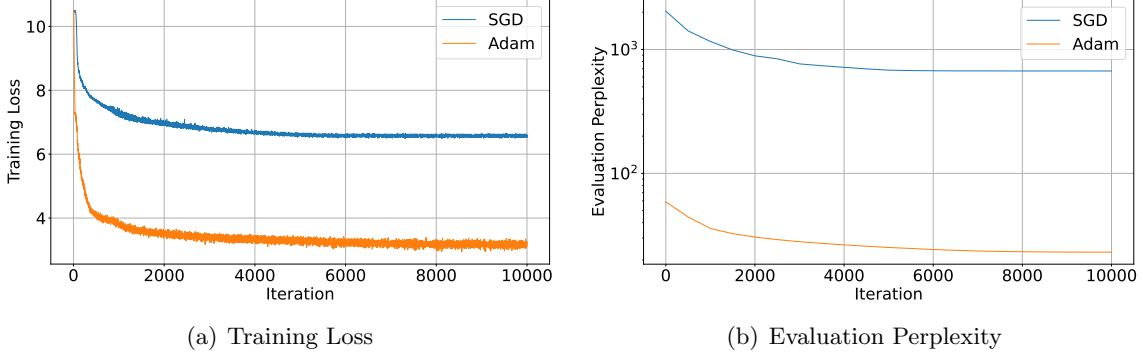


Figure 2: Comparison of SGD and Adam training loss and evaluation perplexity curves on LLaMA 130M model. Clearly, SGD is not converging to any reasonable level of perplexity. The Adam and SGD learning rates are $3e-3$ and 0.1 , respectively. We search with multiple learning rates for SGD, for lower ones the loss decreases even slower and higher ones would cause the training to diverge.

2 Methodology

We begin by reviewing several key techniques used in popular optimizers such as Adam and Muon, which have been shown to accelerate pretraining performance for LLMs. This understanding will be critical for our subsequent minimalist design for a memory-efficient optimizer.

Denote the optimization problem of the LLM pretraining as

$$\min_{\theta=[\theta_1, \dots, \theta_L]} \ell(\theta) := \frac{1}{n} \sum_{i=1}^n \ell(\theta; \xi_i) \quad (2.1)$$

where ℓ is the loss function, usually taken as the cross entropy loss of predicting the next token, $\theta = [\theta_1, \dots, \theta_L]$ is the model trainable parameters, with θ_l the l -th layer, $l = 1, 2, \dots, L$. With attention-based network, we can simply assume that each $\theta_l \in \mathbb{R}^{d_{l,\text{in}} \times d_{l,\text{out}}}$ is a weight matrix, with the input dimension $d_{l,\text{in}}$ and output dimension $d_{l,\text{out}}$. Here ξ_i with $i = 1, \dots, n$ represents training data samples and n is the training data size.

To solve (2.1), vanilla SGD draws a small batch of i.i.d samples $\{\xi_{t,b}\}_{b=1, \dots, B}$ at iteration t and performs update toward the negative stochastic gradient direction:

$$\theta^{t+1} = \theta^t - \eta_t g^t, \quad \text{with} \quad g^t := \frac{1}{B} \sum_{b=1}^B \nabla \ell(\theta^t; \xi_{t,b}) \quad (2.2)$$

where B is batch size and η_t is the learning rate. Although memory-efficient, plain SGD performs poorly in LLM training due to the lack of adaptive scaling (Zhao et al., 2025), and we verify this in Figure 2 where we run SGD and Adam on LLaMA 130M pretraining task (see Section 4 for the details of our experiment settings). Therefore we will not include the perplexity result for SGD in the subsequent experiments.

In contrast, adaptive algorithms such as Adam (Kingma and Ba, 2015) update parameters using a more sophisticated scheme (where \odot represents element-wise product):

$$\begin{aligned} m^t &= \beta_1 m^{t-1} + (1 - \beta_1) g^t, \\ v^t &= \beta_2 v^{t-1} + (1 - \beta_2) g^t \odot g^t, \\ \theta^{t+1} &= \theta^t - \eta_t \frac{m^t}{\sqrt{v^t + \epsilon}}. \end{aligned} \quad (2.3)$$

Numerous theoretical works such as Reddi et al. (2019); Zhang et al. (2022b,a) attempted to explain why Adam outperforms SGD for transformers, though consensus remains elusive. A straightforward decomposition of Adam identifies two essential components.

1. **Gradient Normalization.** The key difference between Adam and SGD is the normalization factor v^t in the denominator. One could first normalize each element of SGD, resulting in the sign-SGD update as follows:

$$\theta^{t+1} = \theta^t - \eta_t \frac{g^t}{\sqrt{g^t \odot g^t}} = \theta^t - \eta_t \text{sign}(g^t) \quad (2.4)$$

where sign stands for taking the sign for each element.

2. **Exponential Moving Average (EMA).** The stochasticity of the mini-batch sample $\{\xi_{t,b}\}_{b=1,\dots,B}$ of g^t could be smoothed by taking the exponential moving average (EMA) for both the numerator and denominator for the update (2.4), resulting in the following Adam update of the numerator and denominator:

$$m^t = \beta_1 m^{t-1} + (1 - \beta_1) g^t, \quad v^t = \beta_2 v^{t-1} + (1 - \beta_2) g^t \odot g^t. \quad (2.5)$$

This leads to the central question: **How much of Adam’s benefit arises from gradient normalization versus EMA?** We note that gradient normalization does not require maintaining state, whereas EMA does. Therefore, in the next sections, we will examine each of these components separately and discuss their effectiveness. We will start from the gradient normalization, as the EMA step will introduce extra memory no matter how hard we compress it. Then we will discuss how to use EMA in a more memory-friendly way to further boost the performance of the optimizer.

2.1 Gradient normalization

Gradient normalization is a critical component for large-scale, efficient pretraining, and has remained indispensable even in recent (near)-stateless optimizers (Ma et al., 2024; Huang et al., 2025a; Zhu et al., 2024). It is known to accelerate escape from saddle points (Levy, 2016; Murray et al., 2019), improve the effective smoothness of the objective (when the Hessian norm is upper bounded in terms of the gradient norm) (Zhang et al., 2020a; Kunstner et al., 2023), stabilize gradient distributions (Ma et al., 2024), and provide robustness to heavy-tailed noise (Sun et al., 2024).

In this section, we build upon the framework presented in Bernstein and Newhouse (2024); Pethick et al. (2025) to explore a family of gradient normalization methods within the context of trust-region steepest descent. Denote G^t the stochastic gradient of current iteration (we switch to upper letters since we assume the weight blocks θ_l in (2.1) are matrices). It has been observed that different normalization techniques arise from using different matrix norms in the following steepest descent formulation:

$$\Theta^{t+1} = \Theta^t + \eta_t \Delta^t, \quad \text{where } \Delta^t = \underset{\|\Delta\| \leq \rho}{\text{argmin}} \langle G^t, \Delta \rangle \quad (2.6)$$

where $G^t \in \mathbb{R}^{m \times n}$ denotes the (stochastic) gradient at iteration t . In particular, we use $\|A\|_{p \rightarrow q}$ to represent the operator norm of matrix A induced by vector norm ℓ_p and ℓ_q , i.e., $\|A\|_{p \rightarrow q} :=$

$\max_{\|x\|_p \leq 1} \|Ax\|_q$. We can derive the following results based on [Bernstein and Newhouse \(2024\)](#)¹:

$$\begin{aligned}
 \operatorname{argmin}_{\|\Delta\|_{2 \rightarrow 2} \leq 1} \langle G, \Delta \rangle &= -UV^\top, \text{ where } G = U\Sigma V^\top \text{ is the SVD,} \\
 \operatorname{argmin}_{\|\Delta\|_{1 \rightarrow 2} \leq 1} \langle G, \Delta \rangle &= - \left[\frac{\operatorname{col}_1(G)}{\|\operatorname{col}_1(G)\|}, \dots, \frac{\operatorname{col}_n(G)}{\|\operatorname{col}_n(G)\|} \right], \\
 \operatorname{argmin}_{\|\Delta\|_{2 \rightarrow \infty} \leq 1} \langle G, \Delta \rangle &= - \begin{bmatrix} \frac{\operatorname{row}_1(G)}{\|\operatorname{row}_1(G)\|} \\ \dots \\ \frac{\operatorname{row}_m(G)}{\|\operatorname{row}_m(G)\|} \end{bmatrix}, \\
 \operatorname{argmin}_{\|\Delta\|_{1 \rightarrow \infty} \leq 1} \langle G, \Delta \rangle &= -\operatorname{sign}(G),
 \end{aligned} \tag{2.7}$$

which we refer to as *singular-value*, *column-wise*, *row-wise* and *sign normalization*, respectively. Here we assume that m is the input dimension and n is the output dimension, therefore row- and column-normalizations correspond to normalizing along the input and output dimensions, respectively.

It is worth mentioning that multiple existing works can be summarized in this gradient normalization framework. For example, Sign-SGD/Adam utilize $\|\cdot\|_{1 \rightarrow \infty}$ (sign normalization) to achieve gradient normalization, Muon ([Jordan et al., 2024](#)) utilizes $\|\cdot\|_{2 \rightarrow 2}$ norm (singular-value normalization), whereas SCION ([Pethick et al., 2025](#)) and SlimAdam ([Kalra et al., 2025](#)) apply different norms for different layers to achieve better performance.

Computational cost of different normalizations. In terms of the computational cost, the normalization techniques discussed in (2.7) can be quite different. In particular, singular-value normalization requires computing full SVD, which is the most time consuming compared to the rest. Even though efficient approximation methods of SVD has been studied in [Jordan et al. \(2024\)](#); [Ma et al. \(2024\)](#) (e.g., the Newton-Schulz (NS) procedure), they are still much more time consuming as compare with the other three normalization techniques, see Table 1 for a test on the time required for different normalizations².

dimension d	1024	2048	4096
singular-value	79.77	354.27	1958.66
singular-value (NS)	6.03	7.00	14.41
column-wise	0.10	0.12	0.17
row-wise	0.09	0.11	0.13
sign	0.03	0.03	0.03

Table 1: Time (ms) consumed by each of the normalization methods on a torch matrix tensor with dimension $d_{\text{in}} = d_{\text{out}} = d$, testing on a single NVIDIA A40 GPU. Here the singular-value normalization are computed both exactly (first row, using `torch.linalg.svd` directly) and inexactly using Newton-Schulz (NS) iteration (second row, see [Jordan et al. \(2024\)](#) for details)⁴.

¹It is established in [Bernstein and Newhouse \(2024\)](#) that

$$\operatorname{argmin}_{\|\Delta\| \leq \rho} \langle G, \Delta \rangle = \frac{\rho\nu}{\|G\|_*} \operatorname{argmin}_x \langle G, \Delta \rangle + \frac{\nu}{2} \|\Delta\|^2$$

which indicates that we can also put all the normalization in the context of quadratic minimization.

²In all following experiments, we conduct singular-value normalization with the Newton-Schulz (NS) procedure as in [Jordan et al. \(2024\)](#); [Ma et al. \(2024\)](#).

⁴The difference of column- and row-wise normalization may originate from the way PyTorch stores tensors with strides, see [this link](#).

Experimental comparison of SGD with different gradient normalizations. We conduct the preliminary experiment of pretraining LLaMA models (See Section 4 for the experiment setting) using SGD (2.6) with different normalizations applied to all the layers as specified in (2.7). We report the pretraining perplexities in Table 2, and we notice that all the normalizations improve over SGD, however none of them alone could match the performance of Stable-SPAM (which is a stabilized version of Adam) or Muon, two of the state-of-the-art algorithms. In particular, the four normalization methods can be categorized into two groups based on their performance: singular-value and column-wise normalization achieve better results than row-wise and sign normalization. We thus proceed with the group of normalizations with better performance, namely the singular-value and column-wise normalizations.

	60M	130M	350M
Tokens	1.4B	2.6B	7.8B
Adam	30.05	23.13	18.77
Stable-SPAM	28.77	22.20	16.80
Muon	28.86	22.20	16.70
singular-value	34.15	25.25	18.73
column-wise	39.89	28.85	20.38
row-wise	79.27	37.67	21.63
sign	54.36	40.42	27.95

Table 2: Preliminary experiments results (perplexity) of pretraining LLaMA models on C4 dataset, using different norms for steepest gradient descent (2.6) methods as specified in (2.7). For the singular-value normalization, we use the inexact Newton-Schulz (NS) iteration (again see Jordan et al. (2024) for details) for fast approximation.

2.2 Momentum in the last layer

First-order momentum (m^t in (2.3)) has been shown to effectively reduce the variance toward the true gradients; see Liu et al. (2020); Cutkosky and Mehta (2020). Although second-order momentum is used in adaptive optimizers such as Adam and RMSprop, more recent optimizers such as Muon have demonstrated remarkable success without second-order momentum. It is worth noticing that momentum is the major factor that introduces memory overhead in optimizer states, therefore we only consider first-order momentum in our optimizer design. Based on a minimalist optimizer design principle, we plan to investigate whether first-order momentum can be *selectively* used among different layers, while still leading to performance improvements without significantly increasing memory overhead.

Layer-wise gradient variance. Existing works already show the effectiveness of momentum in reducing variances (Liu et al., 2020; Cutkosky and Mehta, 2020). Naturally, if the gradients for different layers have different variances, we could achieve both memory efficiency and variance reduction by applying momentum to the layers with large variances. In the next paragraphs, we identify the layer-wise gradient variances and determine the most important layer that provides the largest performance gain when incorporating momentum; we also justify the effectiveness of different momentum parameters for different layers using a convergence analysis theory in Theorem 2.1.

We first perform a simple experiment on LLaMA 130M to check the gradient variance of different layers. To estimate the gradient variance, one needs to obtain the full gradient (by using the entire training dataset) which is not feasible in practice. Instead, we take a much larger training data batch

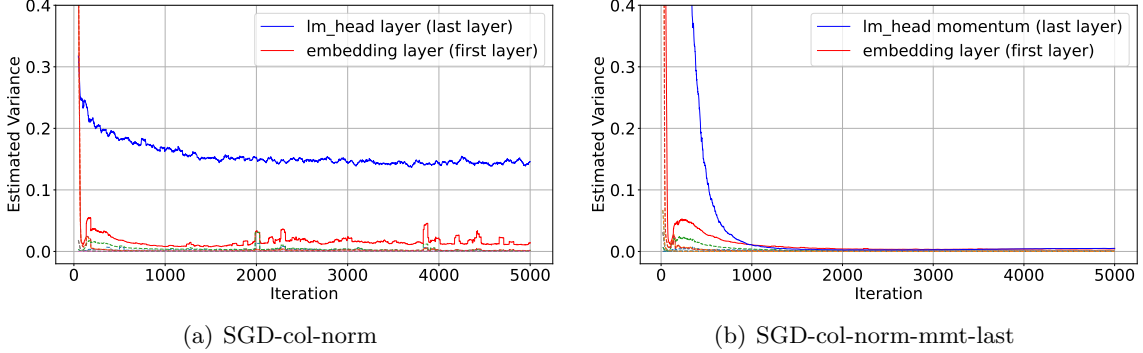


Figure 3: Estimated variance of the stochastic gradients (and momentum when applicable) for different layers in two methods (smoothed by 50 iterations window). We observe that when running SGD with column-wise normalization (SGD-col-norm, left plot), the variance of the last layer (lm_head) is largest for most of the time, following by the variance of the first layer (embedding) and other layers. After applying momentum to the last layer (SGD-col-norm-mmt-last, right plot), the variance of the momentum of last layer (lm_head momentum) decreases to a very low level. Interestingly, the variance of the first layer in plot (b) is also smaller than the one in plot (a).

as input⁵ to estimate the true gradient. The experiment results of running SGD with column-wise normalization (SGD-col-norm) and SGD-col-norm with last layer momentum are shown in Figure 3. Interestingly, we observe that the variance of the last layer is the largest among all the layers during the training time, necessitating a specific treatment for the last layer to reduce the variance.

Next, we show theoretically that momentum helps the most for the layers with larger gradient variances. We inspect the theoretical property of applying SGD with momentum (SGD-M) to the LLM optimization problem (2.1). Note that here we did not consider column-wise normalization for ease of theoretical analysis. Consider the following SGD-M algorithm to solve (2.1) ($m_l^0 = 0$ and θ^1 is randomly initialized):

$$\begin{aligned} m_l^t &= \beta_l m_l^{t-1} + (1 - \beta_l) g^t, \quad g^t = \nabla_{\theta_l} \ell(\theta^t; \xi_t) \\ \theta_l^{t+1} &= \theta_l^t - \eta_l m_l^t \end{aligned} \quad (2.8)$$

where $t = 1, 2, \dots, T$ is the iteration counter; $l = 1, \dots, L$ represents different layers, i.e. we assume different layers contain different momentum with different hyperparameters. We have the following theoretical result (see Appendix A.5 for the proof).

Theorem 2.1. *Suppose $\ell(\theta)$ in (2.1) is lower bounded by ℓ^* , γ -smooth (i.e. $\nabla \ell(\theta)$ is Lipschitz continuous with constant γ), also the stochastic gradient is unbiased $\mathbb{E}_{\xi_t} \nabla_{\theta_l} \ell(\theta^t; \xi_t) = \nabla_{\theta_l} \ell(\theta^t)$ and with bounded variance:*

$$\mathbb{E}_{\xi_t} \|\nabla_{\theta_l} \ell(\theta^t; \xi_t) - \nabla_{\theta_l} \ell(\theta^t)\|^2 \leq \sigma_l^2 \quad (2.9)$$

for all $l = 1, \dots, L$ and $t = 0, \dots, T - 1$. With appropriate choice of hyperparameters $\eta_l \geq \eta$ (see (A.20) and (A.23)) and $\beta_l \leq 1 - \delta$ (δ is an absolute constant), we have the following convergence result for update (2.8):

$$\frac{1}{T} \sum_{t=1}^T \sum_{l=1}^L \mathbb{E} \|\nabla_l^t\|^2 \leq \frac{2L\gamma^{3/2} \mathbb{E} \Delta_1}{\delta^2 \sqrt{T}} + \sum_{l=1}^L \left(\frac{1 - \beta_l}{1 + \beta_l} \frac{L\sqrt{\gamma}}{4\sqrt{T}} + \frac{L\gamma^{3/2}}{2\sqrt{T}} + \frac{1 - \beta_l}{\beta_l^3} \frac{\gamma^2}{4LT} \right) \frac{\sigma_l^2}{\delta^2} \quad (2.10)$$

⁵For example, we take the training batch size as 32 and the large batch size as 512.

where $\Delta_1 = \ell(\theta^1) - \ell^*$.

Remark 2.1. *Theorem 2.1 suggests that by taking different β_l for different layers $l = 1, \dots, L$, the convergence could be improved. The second term of the right-hand side of (2.10) takes the form*

$$f(x) = \frac{1-x}{1+x} + c \frac{1-x}{x^3}, \quad c := \frac{\gamma}{L^2 T^{3/2}}$$

where x represents the layer-wise momentum hyperparameter β_l . It is straightforward to verify that $f(x)$ is decreasing in $(0, 1 - \delta]$, therefore an optimal strategy is to pick $\beta_l = 1 - \delta$. However from a memory-efficient point of view, only $\beta_l = 0$ saves the memory of momentums.

Now, if σ_l (variance of the gradient of the l -th layer) is significantly higher than other layers, then taking β_l higher than other layers will result in better convergence, which is consistent with our experimental findings. On the other hand, if σ_l is close to zero, taking $\beta_l = 0$ will provide memory-efficiency without harming the convergence too much. In particular, if the variances $\sigma_l \approx 0$ for $l = 1, \dots, L - 1$, one could take $\beta_l = 0$ for $l = 1, \dots, L - 1$ and only keep the momentum for the last layer without significantly damaging the convergence rate.

Experiments on different gradient normalization with last-layer-momentum. It is observed in Table 2 that singular-value and column-wise normalization obtains better performance than the other normalizations for pretraining. We conduct another simple experiment to check the performance of the two types of normalization with last-layer-momentum. The results are summarized in Table 3, from which we observe that as the model size gets larger, both singular-value and column-wise normalizations + last-layer-momentum are matching Muon’s performance, and we choose column-wise due to the computational time concern in view of Table 1.

Model Size	60M	130M	350M
Tokens	1.4B	2.6B	7.8B
Muon	28.86	22.20	16.70
Singular-val + last-layer-momentum	31.20	22.33	16.67
Column-wise + last-layer-momentum (ours)	30.81	22.57	16.32

Table 3: Evaluation perplexity of two normalizations (singular-value and column-wise) when combined with last-layer-momentum.

3 Proposed Algorithm

We now introduce our proposed optimizer, **SCALE**, detailed in Algorithm 1. The design of **SCALE** is motivated by empirical insights from our preceding experiments, which highlighted the importance of stabilizing updates in the last layer and controlling gradient scale via column-wise normalization. Accordingly, **SCALE** integrates two components: column-wise normalization of gradients and momentum updates restricted to the last layer. Despite its simplicity, **SCALE** is highly effective and requires only minimal modifications to standard implementations of Adam—typically just a few additional lines of code. As we will demonstrate, this lightweight design allows **SCALE** to outperform state-of-the-art baselines such as Adam and achieve performance competitive with Stable-SPAM and Muon, while using substantially less memory.

Connection to existing works. We now give a discussion on the connection of the proposed method to existing works. The proposed algorithm utilizes column-wise normalization, which is also discussed in Pethick et al. (2025). In particular, Pethick et al. (2025) uses momentum for all

Algorithm 1 SCALE: Stochastic Column-normalized Last-layer Momentum

Input: Initialized trainable parameters θ^0 , hyperparameters β_t and $\eta_{t,l}$.
for $t = 0, 1, \dots, T - 1$ **do**
 Sample mini-batch data $\{\xi_{t,b}\}_{b=1,\dots,B}$;
 for Layers $l = 1, \dots, L$ **do**
 Compute the stochastic gradient $g_l^t := \frac{1}{B} \sum_{b=1}^B \nabla_{\theta_l} \ell(\theta^t; \xi_{t,b})$;
 if $l = L$ (last layer) **then**
 $m_l^t = \beta_t m_l^{t-1} + (1 - \beta_t) \nabla_{\theta_l} \ell(\theta^t; \xi_t)$;
 else
 $m_l^t = \nabla_{\theta_l} \ell(\theta^t; \xi_t)$ (record the gradient directly);
 end if
 $\theta_l^{t+1} = \theta_l^t - \eta_l \mathcal{C}(m_l^t)$ where \mathcal{C} is the column-wise normalization;
 end for
end for
Output: Trained model θ^T .

the layers, also singular-value normalization for most of layers except for the last layer, where they also propose an option of column-wise normalization (since Pethick et al. (2025) denotes the weight matrices as $W \in \mathbb{R}^{d_{\text{out}} \times d_{\text{in}}}$, their row-wise normalization is the same operation as our column-wise normalization); Our method also differs from SWAN (Ma et al., 2024) in the following aspects: first, SWAN utilizes both the row-wise and singular-value normalization while our method only utilizes column-wise normalization, indicating certain redundancy in existing works that apply multiple normalizations; second, SWAN applies Adam for the embedding and LM head layers (the first and last layers) which increases the memory overhead, whereas our approach only introduces first-order momentum for the last layer. We summarize the techniques used in different papers in Table 4.

Convergence of Algorithm 1. We remark here that the convergence provided in Pethick et al. (2025, Section 5) could be adopted to provide a convergence analysis for Algorithm 1, since Algorithm 1 differs from the general framework of Pethick et al. (2025, Algorithm 2) only by the fact that Algorithm 1 applies different momentum for different layers. However, directly applying such kinds of analysis will not be able to explain why using either normalization or momentum is advantageous as compared to vanilla SGD, we choose not to present such a proof.

4 Experiments

In this section, we test the proposed SCALE algorithm for LLM pretraining. We test on pretraining LLaMA (60M, 130M, 350M, 1B, 7B) models on the C4 (Colossal Clean Crawled Corpus) dataset (Raffel et al., 2020).

Baselines. We compare the proposed SCALE with Adam, Stable-SPAM, Muon, GaLore, Fira, APOLLO(-Mini) and SWAN (see Section 1.1 for a more detailed introduction of these works). Stable-SPAM and Muon provide the better pretraining perplexities than Adam (Huang et al., 2025a; Jordan et al., 2024; Glentis et al., 2025). GaLore, Fira and APOLLO(-Mini) are memory-efficient optimizers that project the gradients to low rank. SWAN is an optimizer that uses both singular-value and row-wise normalized SGD except for the first and last layers, and it can achieve state-of-the-art⁶. For Adam, Stable-SPAM, GaLore and Fira, we record their performance from

⁶We copy SWAN’s result directly from Ma et al. (2024) since we cannot replicate the result exactly due to code unavailability.

Methods	Sign	Col-wise	Row-wise	Singular-val	1st order EMA	2nd order EMA	Memory (7B)
SGD							13.48
Adafactor						✓ [†]	13.48
Adam	✓				✓	✓	40.43
Muon				✓	✓		26.95
SWAN			✓	✓		*	14.52
SCALE		✓			Last Layer		13.74

[†]: Adafactor only records the 2nd order EMA of the column and row norms, effectively reducing the memory from $d_{\text{in}} \times d_{\text{out}}$ to $d_{\text{in}} + d_{\text{out}}$

*: SWAN applies Adam for the first and last layer, following the practice of GaLore (see [Ma et al. \(2024, Appendix J\)](#)).

Table 4: A summary of building components of related methods. “Sign”, “Col-wise”, “Row-wise” and “Singular-val” correspond to four normalizations in (2.7), respectively. “1st order EMA” and “2nd order EMA” stand for first and second order EMA/momentum. The last column records the memory (GB) of weights and optimizer states required for applying the corresponding methods for LLaMA 7B training (see Appendix A.1 for the details of the estimation).

[Glentis et al. \(2025\)](#), where a comprehensive benchmark is conducted for these methods.

It is worth noticing that GaLore, Fira, APOLLO(-Mini) and SWAN run Adam for the first and last layers for stable training. For the 60M model the first and last layers contain over 50% of the total network parameters, and around 40% for 130M model. For the 350M this goes down to less than 20% and for the 1B to about 10%. Therefore, for smaller models these methods have limited memory savings as compared to Adam, which trains a significant percentage of the network parameters.

Hyperparameters. For all LLaMA experiments, we follow [Zhao et al. \(2024\)](#) and set the sequence length to 256 and the batch size to 512, train using BF16 format and report evaluation perplexity as our metric. We also use a cosine learning rate with linear warm-up for the first 10% of the iterations. For low-rank optimizers (GaLore, Fira and APOLLO) we follow their suggested hyperparameters (including the rank) but tune the learning rates. For Muon we follow the implementation from [Liu et al. \(2025\)](#). For all the implemented methods, we conduct a hyperparameter search via wandb sweeps (see Appendix A.2 for details).

Results for 60M–1B models. We report the results of the evaluation perplexity in Table 5. We can see that the proposed algorithm outperforms existing memory efficient optimizers, also (nearly) matches the performance of Stable-SPAM and Muon, especially for larger models, with only 35–65% of the memory. We also contrast the performance with the memory consumed in Figure 1, where we can see that the proposed method is indeed at the Pareto frontier for optimal memory usage while maintaining the (near) state-of-the-art performance. This makes it a strong candidate for large-scale pretraining under memory constraints⁷. It also makes our method a minimalist baseline for benchmarking more sophisticated optimizers.

Results for 7B model. We report the results of the evaluation perplexity in Table 6. Due to limited computational resources, we run a single experiment for SCALE with learning rate 1e-4 on 8×NVIDIA H200 141G GPUs. Following [Zhu et al. \(2025\)](#), we train for a total of 19.7B tokens, corresponding to 150K steps. We only compare with APOLLO(-Mini) which is the only baseline

⁷Notice that we construct our optimizer step by step via a minimalist design, and we already conduct the ablations throughout our journey (see Table 2 and 3, also Figure 3). We do not conduct further ablation studies in this section, but we include experiments on the learning rate sensitivity in Appendix A.4.

Model Size	60M	130M	350M	1B
Tokens	1.4B	2.6B	7.8B	13.1B
Adam [†]	30.05 (0.35G)	23.13 (0.81G)	18.77 (2.21G)	16.52 (8.04G)
Stable-SPAM [†]	28.77 (0.35G)	22.20 (0.81G)	16.80 (2.21G)	13.97 (8.04G)
Muon	28.86 (0.23G)	22.20 (0.54G)	16.70 (1.47G)	14.18 (5.36G)
GaLore [†]	34.58 (0.28G)	25.31 (0.61G)	19.37 (1.59G)	15.57 (4.76G)
Fira [†]	30.34 (0.28G)	22.96 (0.61G)	16.82 (1.59G)	15.10 (4.76G)
SWAN*	30.00 (0.25G)	22.83 (0.46G)	17.14 (1.00G)	14.42 (3.20G)
APOLLO	30.94 (0.28G)	22.93 (0.61G)	16.75 (1.59G)	14.20 (4.76G)
APOLLO-Mini	31.85 (0.25G)	23.63 (0.46G)	17.11 (1.00G)	14.13 (3.20G)
SCALE (ours)	30.81 (0.15G)	22.57 (0.32G)	16.32 (0.80G)	14.25 (2.81G)

Table 5: Experiment results for pretraining LLaMA models on C4 dataset. The result marked * is from [Ma et al. \(2024\)](#). The results marked [†] are from [Glentis et al. \(2025\)](#).

that reports the results for 7B model (with BF16 precision). From the table, we conclude that **SCALE** outperforms APOLLO(-Mini) in terms of both final evaluation perplexity and memory.

Steps	40K	80K	120K	150K	
Tokens	5.2B	10.5B	15.7B	19.7B	
APOLLO [†]	(16.14G)	17.55	14.39	13.23	13.02
APOLLO-Mini [†]	(14.53G)	18.03	14.60	13.32	13.09
SCALE (ours)	(13.74G)	17.99	14.57	12.86	12.59

Table 6: Experiment results for pretraining 7B LLaMA model on C4 dataset. The results marked [†] are from [Zhu et al. \(2025\)](#).

5 Conclusion

In this paper, we design a memory-efficient optimizer using a minimalist approach. The proposed algorithm utilizes the building blocks that lead to the success of Adam but further refines them to make it more memory efficient. We motivate each of our construction steps by theoretical or experimental tests. The resulting algorithm, **SCALE**, achieves superior pretraining performance while only requires 35-45% of Adam memory. This makes the proposed algorithm a strong candidate for large-scale pretraining under memory constraints, as well as a minimalist baseline for benchmarking more sophisticated optimizers.

References

- J. Bernstein and L. Newhouse. Old optimizer, new norm: An anthology. *arXiv preprint arXiv:2409.20325*, 2024. (Cited on pages 3, 5, and 6.)
- X. Chen, K. Feng, C. Li, X. Lai, X. Yue, Y. Yuan, and G. Wang. Fira: Can we achieve full-rank training of llms under low-rank constraint? *arXiv preprint arXiv:2410.01623*, 2024. (Cited on page 2.)
- A. Cutkosky and H. Mehta. Momentum improves normalized sgd. In *International conference on machine learning*, pages 2260–2268. PMLR, 2020. (Cited on page 7.)
- A. Glentis, J. Li, Q. Shang, A. Han, I. Tsaknakis, Q. Wei, and M. Hong. Scalable parameter and memory efficient pretraining for llm: Recent algorithmic advances and benchmarking. *arXiv preprint arXiv:2505.22922*, 2025. (Cited on pages 10, 11, and 12.)
- A. Han, J. Li, W. Huang, M. Hong, A. Takeda, P. Jawanpuria, and B. Mishra. SLTrain: a sparse plus low rank approach for parameter and memory efficient pretraining. In *The Thirty-eighth Annual Conference on Neural Information Processing Systems*, 2024. URL <https://openreview.net/forum?id=MXze4H7opg>. (Cited on page 15.)
- G. Hinton, N. Srivastava, and K. Swersky. Neural networks for machine learning lecture 6a overview of mini-batch gradient descent. *Cited on*, 14(8):2, 2012. (Cited on page 1.)
- T. Huang, H. Hu, Z. Zhang, G. Jin, X. Li, L. Shen, T. Chen, L. Liu, Q. Wen, Z. Wang, et al. Stable-spam: How to train in 4-bit more stably than 16-bit adam. *arXiv preprint arXiv:2502.17055*, 2025a. (Cited on pages 3, 5, 10, and 17.)
- T. Huang, Z. Zhu, G. Jin, L. Liu, Z. Wang, and S. Liu. SPAM: Spike-aware adam with momentum reset for stable LLM training. In *The Thirteenth International Conference on Learning Representations*, 2025b. URL <https://openreview.net/forum?id=L9eBxTCpQG>. (Cited on page 3.)
- K. Jordan, Y. Jin, V. Boza, J. You, F. Cesista, L. Newhouse, and J. Bernstein. Muon: An optimizer for hidden layers in neural networks, 2024. URL <https://kellerjordan.github.io/posts/muon/>. (Cited on pages 2, 3, 6, 7, 10, and 16.)
- D. S. Kalra, J. Kirchenbauer, M. Barkeshli, and T. Goldstein. When can you get away with low memory adam? *arXiv preprint arXiv:2503.01843*, 2025. (Cited on pages 3 and 6.)
- D. P. Kingma and J. Ba. Adam: A Method for Stochastic Optimization. In *3rd International Conference on Learning Representations (ICLR)*, 2015. (Cited on pages 1 and 4.)
- F. Kunstner, J. Chen, J. W. Lavington, and M. Schmidt. Noise is not the main factor behind the gap between sgd and adam on transformers, but sign descent might be. In *The Eleventh International Conference on Learning Representations*, 2023. URL <https://openreview.net/forum?id=a65YK0cqH8g>. (Cited on page 5.)
- K. Y. Levy. The power of normalization: Faster evasion of saddle points. *arXiv preprint arXiv:1611.04831*, 2016. (Cited on page 5.)
- X. Liao, S. Li, Y. Xu, Z. Li, Y. Liu, and Y. He. Galore +: Boosting low-rank adaptation for llms with cross-head projection. *arXiv preprint arXiv:2412.19820*, 2024. (Cited on page 16.)

- H. Liu, Z. Li, D. L. W. Hall, P. Liang, and T. Ma. Sophia: A scalable stochastic second-order optimizer for language model pre-training. In *The Twelfth International Conference on Learning Representations*, 2024. URL <https://openreview.net/forum?id=3xHDeA8Noi>. (Cited on pages 2 and 3.)
- J. Liu, J. Su, X. Yao, Z. Jiang, G. Lai, Y. Du, Y. Qin, W. Xu, E. Lu, J. Yan, et al. Muon is scalable for llm training. *arXiv preprint arXiv:2502.16982*, 2025. (Cited on pages 11 and 16.)
- Y. Liu, Y. Gao, and W. Yin. An improved analysis of stochastic gradient descent with momentum. *Advances in Neural Information Processing Systems*, 33:18261–18271, 2020. (Cited on pages 7 and 18.)
- Q. Luo, H. Yu, and X. Li. Badam: A memory efficient full parameter training method for large language models. *arXiv preprint arXiv:2404.02827*, 2024. (Cited on page 3.)
- C. Ma, W. Gong, M. Scetbon, and E. Meeds. SWAN: Preprocessing sgd enables adam-level performance on llm training with significant memory reduction. *arXiv preprint arXiv:2412.13148*, 2024. (Cited on pages 2, 3, 5, 6, 10, 11, and 12.)
- A. Muhamed, O. Li, D. Woodruff, M. Diab, and V. Smith. GRASS: Compute efficient low-memory llm training with structured sparse gradients. In *Proceedings of the 2024 Conference on Empirical Methods in Natural Language Processing*, pages 14978–15003, 2024. (Cited on page 3.)
- R. Murray, B. Swenson, and S. Kar. Revisiting normalized gradient descent: Fast evasion of saddle points. *IEEE Transactions on Automatic Control*, 64(11):4818–4824, 2019. (Cited on page 5.)
- R. Pan, X. Liu, S. Diao, R. Pi, J. Zhang, C. Han, and T. Zhang. Lisa: layerwise importance sampling for memory-efficient large language model fine-tuning. *Advances in Neural Information Processing Systems*, 37:57018–57049, 2024. (Cited on page 3.)
- T. Pethick, W. Xie, K. Antonakopoulos, Z. Zhu, A. Silveti-Falls, and V. Cevher. Training deep learning models with norm-constrained lmos. *arXiv preprint arXiv:2502.07529*, 2025. (Cited on pages 2, 3, 5, 6, 9, and 10.)
- C. Raffel, N. Shazeer, A. Roberts, K. Lee, S. Narang, M. Matena, Y. Zhou, W. Li, and P. J. Liu. Exploring the limits of transfer learning with a unified text-to-text transformer. *Journal of Machine Learning Research*, 21(140):1–67, 2020. (Cited on page 10.)
- A. V. Ramesh, V. Ganapathiraman, I. H. Laradji, and M. Schmidt. Blockllm: Memory-efficient adaptation of llms by selecting and optimizing the right coordinate blocks. *arXiv preprint arXiv:2406.17296*, 2024. (Cited on page 3.)
- S. J. Reddi, S. Kale, and S. Kumar. On the convergence of adam and beyond. In *International Conference on Learning Representations (ICLR)*, 2019. (Cited on page 5.)
- N. Shazeer and M. Stern. Adafactor: Adaptive learning rates with sublinear memory cost. In *International Conference on Machine Learning*, pages 4596–4604. PMLR, 2018. (Cited on page 3.)
- T. Sun, X. Liu, and K. Yuan. Gradient normalization provably benefits nonconvex sgd under heavy-tailed noise. *arXiv preprint arXiv:2410.16561*, 2024. (Cited on page 5.)
- M. Xu, L. Xiang, X. Cai, and H. Wen. No more adam: Learning rate scaling at initialization is all you need. *arXiv preprint arXiv:2412.11768*, 2024. (Cited on pages 2 and 3.)

- J. Zhang, T. He, S. Sra, and A. Jadbabaie. Why gradient clipping accelerates training: A theoretical justification for adaptivity. In *International Conference on Learning Representations*, 2020a. URL <https://openreview.net/forum?id=BJgnXpVYwS>. (Cited on page 5.)
- J. Zhang, S. P. Karimireddy, A. Veit, S. Kim, S. Reddi, S. Kumar, and S. Sra. Why are adaptive methods good for attention models? *Advances in Neural Information Processing Systems*, 33: 15383–15393, 2020b. (Cited on page 1.)
- Y. Zhang, C. Chen, and Z.-Q. Luo. Does adam converge and when? In *ICLR Blog Track*, 2022a. URL <https://iclr-blog-track.github.io/2022/03/25/does-adam/>. <https://iclr-blog-track.github.io/2022/03/25/does-adam/>. (Cited on page 5.)
- Y. Zhang, C. Chen, N. Shi, R. Sun, and Z.-Q. Luo. Adam can converge without any modification on update rules. *Advances in neural information processing systems*, 35:28386–28399, 2022b. (Cited on page 5.)
- Y. Zhang, C. Chen, Z. Li, T. Ding, C. Wu, Y. Ye, Z.-Q. Luo, and R. Sun. Adam-mini: Use fewer learning rates to gain more. *arXiv preprint arXiv:2406.16793*, 2024. (Cited on pages 2 and 3.)
- J. Zhao, Z. Zhang, B. Chen, Z. Wang, A. Anandkumar, and Y. Tian. Galore: Memory-efficient LLM training by gradient low-rank projection. In *Forty-first International Conference on Machine Learning*, 2024. (Cited on pages 2, 11, and 15.)
- R. Zhao, D. Morwani, D. Brandfonbrener, N. Vyas, and S. M. Kakade. Deconstructing what makes a good optimizer for autoregressive language models. In *The Thirteenth International Conference on Learning Representations*, 2025. (Cited on pages 1, 3, and 4.)
- H. Zhu, Z. Zhang, W. Cong, X. Liu, S. Park, V. Chandra, B. Long, D. Z. Pan, Z. Wang, and J. Lee. Apollo: Sgd-like memory, adamw-level performance, 2024. URL <https://arxiv.org/abs/2412.05270>. (Cited on pages 2 and 5.)
- H. Zhu, Z. Zhang, W. Cong, X. Liu, S. Park, V. Chandra, B. Long, D. Z. Pan, Z. Wang, and J. Lee. APOLLO: SGD-like memory, adamw-level performance. In *Eighth Conference on Machine Learning and Systems*, 2025. URL <https://openreview.net/forum?id=mJrPkdcZDj>. (Cited on pages 3, 11, and 12.)

A Appendix

A.1 Details of memory estimation for 1B and 7B models

Here we compute the memory estimate for both 1B and 7B LLaMA models. We only compute the major parameters, including embedding layers, attention and MLP layers. We follow prior works (Zhao et al., 2024; Han et al., 2024) in estimating the memory using `bf16` format, where each floating point number occupies 2 bytes.

7B model: Pre-last layers include 6.607B parameters and last layer includes 0.131B parameters, which in total leads to 6.738B parameters.

- **SGD:** Only the parameter states are stored, which amount to 13.476G memory.
- **Adafactor:** Apart from the parameter states, Adafactor stores a row-wise and column-wise momentum, which is 0.005G memory. In total, Adafactor requires 13.481G memory.

- **Adam**: Apart from the parameter states, Adam/AdamW store first and second order momentum, which costs 26.952G. In total, Adam/AdamW requires 40.428G memory.
- **APOLLO**: Apart from the parameter states, APOLLO stores first-order and second-order momentum in the low-rank subspace of 256, which in total costs 16.144G.
- **APOLLO-Mini**: Apart from the parameter states, APOLLO-Mini sets rank to be 1, which leads to a total memory of 14.531G.
- **Muon**: Apart from the parameter states, Muon stores first-order momentum, which costs 13.476G. In total, Muon requires 26.952G memory.
- **SWAN**: Apart from the parameter states, SWAN additionally stores first-order and second-order momentum of the first and last layer, which costs 1.048G. In total, SWAN requires 14.524G.
- **SCALE (Our method)**: Apart from parameter states, SCALE additionally stores first-order momentum of last-layer weight, which costs 0.262G. In total, SCALE requires 13.738G memory.

1B model: Pre-last layers include 1.273B parameters and last layer includes 0.066B parameters, which in total leads to 1.339B parameters.

- **SGD**: Only the parameter states are stored, which amount to 2.678G memory.
- **Adafactor**: Apart from the parameter states, Adafactor stores a row-wise and column-wise momentum, which is 0.002G memory. In total, Adafactor requires 2.68G memory.
- **Adam**: Apart from the parameter states, Adam/AdamW store first and second order momentum, which costs 5.356G. In total, Adam/AdamW requires 8.034G memory.
- **Muon**: Apart from the parameter states, Muon stores first-order momentum, which costs 2.678G. In total, Muon requires 5.356G memory.
- **SWAN**: Apart from the parameter states, SWAN additionally stores first-order and second-order momentum of the first and last layer, which costs 0.524G. In total, SWAN requires 3.202G.
- **SCALE (Our method)**: Apart from parameter states, SCALE additionally stores first-order momentum of last-layer weight, which costs 0.131G. In total, SCALE requires 2.809G memory.

A.2 Details of the experiments

We performed wandb sweeps for all methods we tested up to models of size 350M, searching learning rates within $\{0.00005, 0.0001, 0.0003, 0.0005, 0.001, 0.003, 0.005, 0.01\}$. For the 1B model, due to resource constraints we manually tune the learning rates using as starting point the optimal learning rate from the 350M sweep. For SCALE, we use learning rate $1e-3$ for models sizes 60M, 130M and 350M, $2e-4$ for the 1B and $1e-4$ for the 7B model. In addition, our reported result for the 1B model uses the same learning rate scaling technique used by Muon (Liu et al., 2025), as we find to result to a minor gain; without it, the achieved perplexity for the 1B model is 14.34. Also, we set the last layer’s momentum parameter $\beta = 0.9$, being a common choice for first order momentum. In addition, for all vector parameters we employ the Adam optimizer, following Jordan et al. (2024); Liao et al. (2024). This does not influence the memory usage because the vector parameters are orders of magnitude smaller in size compared to the matrix parameters.

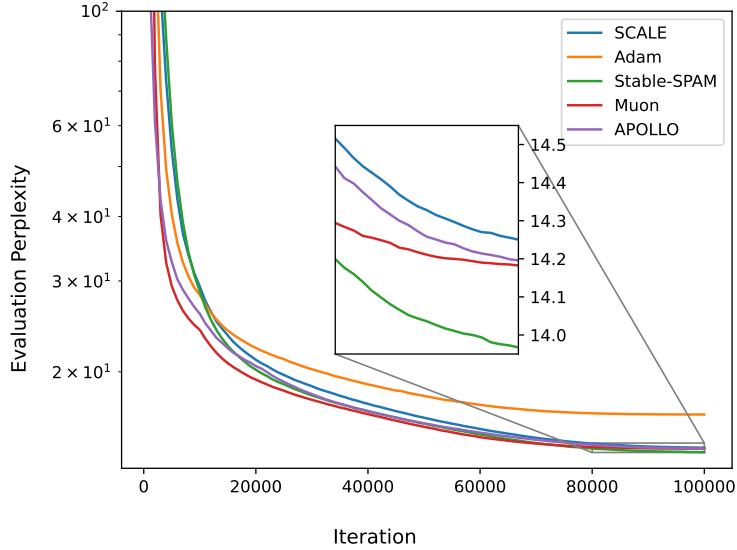


Figure 4: The evaluation perplexity curves of different methods on LLaMA 1B pretraining. Note that Muon is converging fastest at the beginning stage, while SCALE, Stable-SPAM and APOLLO catch up with Muon in the final stage of training.

A.3 Curves of Training Iteration versus Perplexity

A.4 Learning Rate Sensitivity analysis

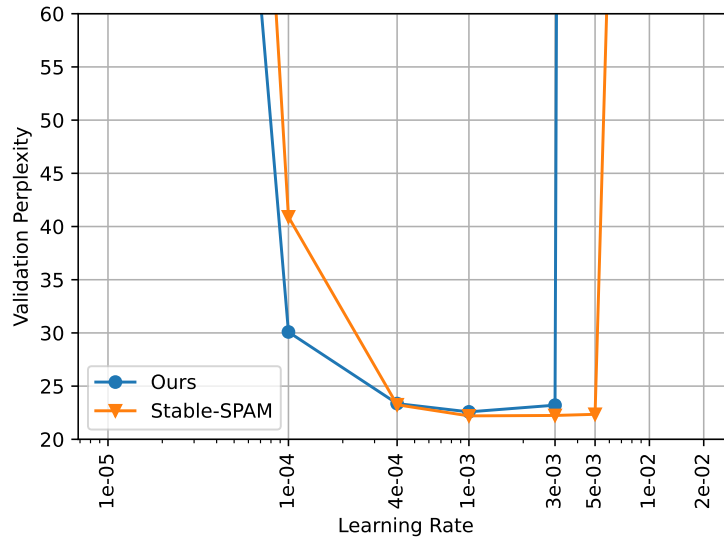


Figure 5: Learning rate sensitivity analysis, comparing Stable-SPAM (a stabilized version of Adam) and our method. Results from the 130M LLaMA model.

In Figure 5 we test the performance of our algorithm, SCALE, with different learning rates and compare it with that of Stable-SPAM (Huang et al., 2025a). We observe that both algorithms

behave similarly with a reasonable range of learning rates.

A.5 Proofs for Section 2.2

In this section, we conduct the proof for Theorem 2.1. The proof follows Liu et al. (2020). First, we have the following lemmas, which are variations of Liu et al. (2020, Lemma 1 and 2).

Lemma A.1. *Suppose that the assumptions in Theorem 2.1 hold. For SGD-M (2.8), we have*

$$\mathbb{E} \left[\left\| m_l^t - (1 - \beta_l) \sum_{i=1}^t \beta_l^{t-i} \nabla_{\theta_l} \ell(\theta^i) \right\|^2 \right] \leq \frac{1 - \beta_l}{1 + \beta_l} (1 - \beta_l^{2t}) \sigma_l^2. \quad (\text{A.1})$$

Proof. It is straightforward to see $m_l^t = (1 - \beta_l) \sum_{i=1}^t \beta_l^{t-i} g_l^i$, where $g_l^i := \nabla_{\theta_l} f(\theta^i; \xi_i)$.

We have

$$\mathbb{E} \left[\left\| m_l^t - (1 - \beta_l) \sum_{i=1}^t \beta_l^{t-i} \nabla_{\theta_l} \ell(\theta^i) \right\|^2 \right] = (1 - \beta_l)^2 \mathbb{E} \left[\left\| \sum_{i=1}^t \beta_l^{t-i} (g_l^i - \nabla_{\theta_l} \ell(\theta^i)) \right\|^2 \right].$$

Therefore

$$\begin{aligned} & \mathbb{E} \left[\left\| m_l^t - (1 - \beta_l) \sum_{i=1}^t \beta_l^{t-i} \nabla_{\theta_l} \ell(\theta^i) \right\|^2 \right] \\ &= (1 - \beta_l)^2 \mathbb{E}_{\xi_1} \mathbb{E}_{\xi_2} \cdots \mathbb{E}_{\xi_t} \left[\left\| \sum_{i=1}^t \beta_l^{t-i} (g_l^i - \nabla_{\theta_l} \ell(\theta^i)) \right\|^2 \right] \\ &= (1 - \beta_l)^2 \mathbb{E}_{\xi_1} \mathbb{E}_{\xi_2} \cdots \mathbb{E}_{\xi_t} \left[\sum_{i=1}^t \sum_{j=1}^t \langle \beta_l^{t-i} (g_l^i - \nabla_{\theta_l} \ell(\theta^i)), \beta_l^{t-j} (g_l^j - \nabla_{\theta_l} \ell(\theta^j)) \rangle \right]. \end{aligned}$$

Due to unbiasedness of stochastic gradients, the cross terms cancel, therefore we have

$$\begin{aligned} & \mathbb{E} \left[\left\| m_l^t - (1 - \beta_l) \sum_{i=1}^t \beta_l^{t-i} \nabla_{\theta_l} \ell(\theta^i) \right\|^2 \right] \\ &= (1 - \beta_l)^2 \sum_{i=1}^t \beta_l^{2(t-i)} \mathbb{E}_{\xi_1} \mathbb{E}_{\xi_2} \cdots \mathbb{E}_{\xi_t} \|g_l^i - \nabla_{\theta_l} \ell(\theta^i)\|^2 \leq \frac{1 - \beta_l}{1 + \beta_l} (1 - \beta_l^{2t}) \sigma_l^2, \end{aligned}$$

for all layers $l = 1, \dots, L$. □

Lemma A.2. *Suppose that the assumptions in Theorem 2.1 hold. For SGD-M (2.8), we have*

$$\mathbb{E} \left[\left\| \frac{1 - \beta_l}{1 - \beta_l^t} \sum_{i=1}^t \beta_l^{t-i} \nabla_{\theta_l} \ell(\theta^i) - \nabla_{\theta_l} \ell(\theta^t) \right\|^2 \right] \leq \sum_{i=1}^{t-1} a_{l,t,i} \mathbb{E} \left[\|\theta^{i+1} - \theta^i\|^2 \right], \quad (\text{A.2})$$

for all layers $l = 1, \dots, L$, where

$$a_{l,t,i} = \frac{\gamma^2 \beta_l^{t-i}}{1 - \beta_l^t} \left(t - i + \frac{\beta_l}{1 - \beta_l} \right). \quad (\text{A.3})$$

Proof. Since

$$\begin{aligned}
& \mathbb{E} \left[\left\| \frac{1 - \beta_l}{1 - \beta_l^t} \sum_{i=1}^t \beta_l^{t-i} \nabla_{\theta_l} \ell(\theta^i) - \nabla_{\theta_l} \ell(\theta^t) \right\|^2 \right] \\
&= \left(\frac{1 - \beta_l}{1 - \beta_l^t} \right)^2 \sum_{i,j=1}^t \mathbb{E} \left[\left\langle \beta_l^{t-i} (\nabla_{\theta_l} \ell(\theta^t) - \nabla_{\theta_l} \ell(\theta^i)), \beta_l^{t-j} (\nabla_{\theta_l} \ell(\theta^t) - \nabla_{\theta_l} \ell(\theta^j)) \right\rangle \right] \\
&\leq \left(\frac{1 - \beta_l}{1 - \beta_l^t} \right)^2 \sum_{i,j=1}^t \beta_l^{2t-i-j} \left(\frac{1}{2} \mathbb{E} \left[\|\nabla_{\theta_l} \ell(\theta^t) - \nabla_{\theta_l} \ell(\theta^i)\|^2 \right] + \frac{1}{2} \mathbb{E} \left[\|\nabla_{\theta_l} \ell(\theta^t) - \nabla_{\theta_l} \ell(\theta^j)\|^2 \right] \right) \\
&= \left(\frac{1 - \beta_l}{1 - \beta_l^t} \right)^2 \sum_{i=1}^t \left(\sum_{j=1}^t \beta_l^{2t-i-j} \right) \frac{1}{2} \mathbb{E} \left[\|\nabla_{\theta_l} \ell(\theta^t) - \nabla_{\theta_l} \ell(\theta^j)\|^2 \right] \\
&\quad + \left(\frac{1 - \beta_l}{1 - \beta_l^t} \right)^2 \sum_{j=1}^t \left(\sum_{i=1}^t \beta_l^{2t-i-j} \right) \frac{1}{2} \mathbb{E} \left[\|\nabla_{\theta_l} \ell(\theta^t) - \nabla_{\theta_l} \ell(\theta^i)\|^2 \right] \\
&= \left(\frac{1 - \beta_l}{1 - \beta_l^t} \right)^2 \sum_{i=1}^t \frac{\beta_l^{t-i} (1 - \beta_l^t)}{1 - \beta_l} \mathbb{E} \left[\|\nabla_{\theta_l} \ell(\theta^t) - \nabla_{\theta_l} \ell(\theta^i)\|^2 \right] \\
&= \frac{1 - \beta_l}{1 - \beta_l^t} \sum_{i=1}^t \beta_l^{t-i} \mathbb{E} \left[\|\nabla_{\theta_l} \ell(\theta^t) - \nabla_{\theta_l} \ell(\theta^i)\|^2 \right] \\
&\leq \frac{1 - \beta_l}{1 - \beta_l^t} \sum_{i=1}^t \beta_l^{t-i} (t - i) \sum_{j=i}^t \mathbb{E} \left[\|\nabla_{\theta_l} \ell(\theta^{j+1}) - \nabla_{\theta_l} \ell(\theta^j)\|^2 \right]
\end{aligned}$$

where we use Cauchy-Schwarz inequality for the first inequality and the last is by AM-GM inequality. Now applying the Lipschitz smoothness assumption, we have

$$\begin{aligned}
& \mathbb{E} \left[\left\| \frac{1 - \beta_l}{1 - \beta_l^t} \sum_{i=1}^t \beta_l^{t-i} \nabla_{\theta_l} \ell(\theta^i) - \nabla_{\theta_l} \ell(\theta^t) \right\|^2 \right] \\
&\leq \frac{1 - \beta_l}{1 - \beta_l^t} \sum_{i=1}^t \beta_l^{t-i} (t - i) \sum_{j=i}^t \gamma^2 \mathbb{E} \left[\|\theta^{j+1} - \theta^j\|^2 \right] \\
&\leq \frac{1 - \beta_l}{1 - \beta_l^t} \sum_{j=1}^{t-1} \left(\sum_{i=1}^j \beta_l^{t-i} (t - i) \right) \gamma^2 \mathbb{E} \left[\|\theta^{j+1} - \theta^j\|^2 \right].
\end{aligned}$$

Now define

$$a'_{l,t,i} = \frac{1 - \beta_l}{1 - \beta_l^t} \gamma^2 \sum_{i=1}^j \beta_l^{t-i} (t - i) = \frac{\gamma^2 \beta_l^t}{1 - \beta_l^t} \left(-(t - 1) - \frac{1}{1 - \beta_l} \right) + \frac{\gamma^2 \beta_l^{t-j}}{1 - \beta_l^t} \left(t - j + \frac{\beta_l}{1 - \beta_l} \right) \leq a_{l,t,i},$$

then we get (A.2). \square

Lemma A.3. For SGD-M (2.8), define the auxiliary sequence by

$$z_l^t := \begin{cases} \theta_l^t & t = 1 \\ \frac{1}{1 - \beta_l} \theta_l^t - \frac{\beta_l}{1 - \beta_l} \theta_l^{t-1} & t \geq 2 \end{cases} \quad (\text{A.4})$$

and denote $z^t = [z_1^t, \dots, z_L^t]$ the entire auxiliary variable at iteration t . Then we have

$$z_i^{t+1} - z_i^t = -\eta_l g_i^t$$

and

$$z_i^t - \theta_i^t = -\frac{\beta_l}{1 - \beta_l} \eta_l m_i^{t-1}.$$

Proof. For $t = 1$, we have (since $m^0 = 0$)

$$z_i^2 - z_i^1 = \frac{1}{1 - \beta_l} \theta_l^2 - \frac{\beta_l}{1 - \beta_l} \theta_l^1 - \theta_l^1 = \frac{1}{1 - \beta_l} (\theta_l^2 - \theta_l^1) = -\eta_l g_l^1.$$

For $t \geq 2$, we have

$$\begin{aligned} z_i^{t+1} - z_i^t &= \frac{1}{1 - \beta_l} (\theta_l^{t+1} - \theta_l^t) - \frac{\beta_l}{1 - \beta_l} (\theta_l^t - \theta_l^{t-1}) \\ &= \frac{1}{1 - \beta_l} (-\eta_l m_l^t) - \frac{\beta_l}{1 - \beta_l} (-\eta_l m_l^{t-1}) \\ &= \frac{1}{1 - \beta_l} (-\eta_l m_l^t + \eta_l \beta_l m_l^{t-1}) \\ &= -\eta_l g_l^t. \end{aligned}$$

For $z_i^t - \theta_i^t$, it can be computed similarly. □

We need the following proposition to show the final convergence of Theorem 2.1.

Proposition A.1. *Suppose that the assumptions in Theorem 2.1 hold. For SGD-M (2.8), we have*

$$\begin{aligned} &\mathbb{E} [\ell(z^{t+1})] \\ &\leq \mathbb{E} [\ell(z^t)] + \rho_0 \left(\sum_{l=1}^L \eta_l \right) \sum_{l=1}^L \left(\eta_l^2 \left(\frac{\beta_l}{1 - \beta_l} \right)^2 \gamma^2 \frac{1 - \beta_l}{1 + \beta_l} \right) \sigma_l^2 + \sum_{l=1}^L \frac{\gamma \eta_l^2}{2} \sigma_l^2 \\ &\quad + \sum_{l=1}^L \left(-\eta_l + \frac{\eta_l}{2\rho_0} + \frac{\gamma \eta_l^2}{2} \right) \mathbb{E} \|\nabla_l \ell(\theta^t)\|^2 + 2\rho_0 \left(\sum_{l=1}^L \eta_l \right) \sum_{l=1}^L \left(\eta_l^2 \left(\frac{\beta_l}{1 - \beta_l} \right)^2 \gamma^2 (1 - \beta_l^{t-1})^2 \mathbb{E} [\|\nabla_l \ell(\theta^t)\|^2] \right) \\ &\quad + 2\rho_0 \left(\sum_{l=1}^L \eta_l \right) \sum_{l=1}^L \left(\eta_l^2 \gamma^2 \left(\frac{1 - \beta_l^t}{1 - \beta_l} \right)^2 \mathbb{E} \left[\left\| \frac{1 - \beta_l}{1 - \beta_l^t} \sum_{i=1}^t \beta_l^{t-i} \nabla_l \ell(\theta^i) - \nabla_l \ell(\theta^t) \right\|^2 \right] \right) \end{aligned} \tag{A.5}$$

where the auxiliary sequence z_l^t is defined by (A.4).

Proof. By Lemma A.3 we have that

$$z_l^{t+1} - z_l^t = -\eta_l g_l^t$$

and

$$z_l^t - \theta_l^t = -\frac{\beta_l}{1 - \beta_l} \eta_l m_l^{t-1},$$

for all $l = 1, 2, \dots, L$.

Now using the Lipschitz smooth of ℓ , we get

$$\begin{aligned}
\mathbb{E}_{\xi_t} [\ell(z^{t+1})] &\leq \ell(z^t) + \mathbb{E}_{\xi_t} [\langle \nabla \ell(z^t), z^{t+1} - z^t \rangle] + \frac{L}{2} \mathbb{E}_{\xi_t} [\|z^{t+1} - z^t\|^2] \\
&= \ell(z^t) + \sum_{l=1}^L \mathbb{E}_{\xi_t} [\langle \nabla_{\theta_l} \ell(z^t), -\eta_l g_l^t \rangle] + \sum_{l=1}^L \frac{\gamma \eta_l^2}{2} \mathbb{E}_{\xi_t} [\|g_l^t\|^2] \\
&= \ell(z^t) + \sum_{l=1}^L [\langle \nabla_{\theta_l} \ell(z^t), -\eta_l \nabla_l \ell(\theta^t) \rangle] + \sum_{l=1}^L \frac{\gamma \eta_l^2}{2} \mathbb{E}_{\xi_t} [\|g_l^t\|^2]
\end{aligned}$$

where we use the unbiasedness of the gradient estimator in the last line. Now we bound the second term as follows:

$$\begin{aligned}
&\mathbb{E} [\langle \nabla_{\theta_l} \ell(z^t), -\eta_l \nabla_l \ell(\theta^t) \rangle] \\
&= \mathbb{E} [\langle \nabla_{\theta_l} \ell(z^t) - \nabla_l \ell(\theta^t), -\eta_l \nabla_l \ell(\theta^t) \rangle] - \eta_l \mathbb{E} \|\nabla_l \ell(\theta^t)\|^2 \\
&\leq \eta_l \frac{\rho_0}{2} \gamma^2 \mathbb{E} \|z^t - \theta^t\|^2 + \left(\frac{\eta_l}{2\rho_0} - \eta_l\right) \mathbb{E} \|\nabla_l \ell(\theta^t)\|^2 \\
&= \eta_l \frac{\rho_0}{2} \sum_l \left(\eta_l^2 \mathbb{E} \left[\left(\frac{\beta_l}{1 - \beta_l} \right)^2 \gamma^2 \|m_l^{t-1}\|^2 \right] \right) + \left(\frac{\eta_l}{2\rho_0} - \eta_l\right) \mathbb{E} \|\nabla_l \ell(\theta^t)\|^2
\end{aligned}$$

where we use Cauchy-Schwarz inequality and ρ_0 is a positive constant to be determined.

Therefore, we get

$$\begin{aligned}
\mathbb{E}_{\xi_t} [\ell(z^{t+1})] &\leq \ell(z^t) + \frac{\rho_0}{2} \left(\sum_{l=1}^L \eta_l \right) \sum_{l=1}^L \left(\eta_l^2 \left(\frac{\beta_l}{1 - \beta_l} \right)^2 \gamma^2 \mathbb{E} \|m_l^{t-1}\|^2 \right) \\
&\quad + \sum_{l=1}^L \left(\frac{\eta_l}{2\rho_0} - \eta_l \right) \mathbb{E} \|\nabla_l \ell(\theta^t)\|^2 + \sum_{l=1}^L \frac{\gamma \eta_l^2}{2} \mathbb{E}_{\xi_t} [\|g_l^t\|^2]
\end{aligned} \tag{A.6}$$

Now from Lemma A.1 we have

$$\begin{aligned}
\mathbb{E} [\|m_l^{t-1}\|^2] &\leq 2\mathbb{E} \left[\left\| m_l^{t-1} - (1 - \beta_l) \sum_{i=1}^{t-1} \beta_l^{t-1-i} \nabla_l \ell(\theta^i) \right\|^2 \right] + 2\mathbb{E} \left[\left\| (1 - \beta_l) \sum_{i=1}^{t-1} \beta_l^{t-1-i} \nabla_l \ell(\theta^i) \right\|^2 \right] \\
&\leq 2\frac{1 - \beta_l}{1 + \beta_l} \sigma_l^2 + 2\mathbb{E} \left[\left\| (1 - \beta_l) \sum_{i=1}^{t-1} \beta_l^{t-1-i} \nabla_l \ell(\theta^i) \right\|^2 \right]
\end{aligned}$$

and

$$\begin{aligned}
\mathbb{E} \left[\left\| \frac{1 - \beta_l}{1 - \beta_l^{t-1}} \sum_{i=1}^{t-1} \beta_l^{t-1-i} \nabla_l \ell(\theta^i) \right\|^2 \right] &\leq 2\mathbb{E} [\|\nabla_l \ell(\theta^t)\|^2] + 2\mathbb{E} \left[\left\| \frac{1 - \beta_l}{1 - \beta_l^{t-1}} \sum_{i=1}^{t-1} \beta_l^{t-1-i} \nabla_l \ell(\theta^i) - \nabla_l \ell(\theta^t) \right\|^2 \right], \\
\mathbb{E} [\|g_l^t\|^2] &\leq \sigma_l^2 + \mathbb{E} [\|\nabla_l \ell(\theta^t)\|^2].
\end{aligned}$$

plug these into (A.6) we get:

$$\begin{aligned}
& \mathbb{E}_{\xi_t} [\ell(z^{t+1})] \\
& \leq \ell(z^t) + \rho_0 \left(\sum_{l=1}^L \eta_l \right) \sum_{l=1}^L \left(\eta_l^2 \left(\frac{\beta_l}{1-\beta_l} \right)^2 \gamma^2 \frac{1-\beta_l}{1+\beta_l} \sigma_l^2 \right) \\
& \quad + \rho_0 \left(\sum_{l=1}^L \eta_l \right) \sum_{l=1}^L \left(\eta_l^2 \left(\frac{\beta_l}{1-\beta_l} \right)^2 \gamma^2 \mathbb{E} \left[\left\| (1-\beta_l) \sum_{i=1}^{t-1} \beta_l^{t-1-i} \nabla_l \ell(\theta^i) \right\|^2 \right] \right) \\
& \quad + \sum_{l=1}^L \left(\frac{\eta_l}{2\rho_0} - \eta_l \right) \mathbb{E} \|\nabla_l \ell(\theta^t)\|^2 + \sum_{l=1}^L \frac{\gamma \eta_l^2}{2} \left(\sigma_l^2 + \mathbb{E} \left[\|\nabla_l \ell(\theta^t)\|^2 \right] \right) \\
& = \ell(z^t) + \rho_0 \left(\sum_{l=1}^L \eta_l \right) \sum_{l=1}^L \left(\eta_l^2 \left(\frac{\beta_l}{1-\beta_l} \right)^2 \gamma^2 \frac{1-\beta_l}{1+\beta_l} \right) \sigma_l^2 + \sum_{l=1}^L \frac{\gamma \eta_l^2}{2} \sigma_l^2 \\
& \quad + \sum_{l=1}^L \left(\frac{\eta_l}{2\rho_0} - \eta_l + \frac{\gamma \eta_l^2}{2} \right) \mathbb{E} \|\nabla_l \ell(\theta^t)\|^2 \\
& \quad + \rho_0 \left(\sum_{l=1}^L \eta_l \right) \sum_{l=1}^L \left(\eta_l^2 \left(\frac{\beta_l}{1-\beta_l} \right)^2 \gamma^2 (1-\beta_l^{t-1})^2 \mathbb{E} \left[\left\| \frac{1-\beta_l}{1-\beta_l^{t-1}} \sum_{i=1}^{t-1} \beta_l^{t-1-i} \nabla_l \ell(\theta^i) \right\|^2 \right] \right) \\
& \leq \ell(z^t) + \rho_0 \left(\sum_{l=1}^L \eta_l \right) \sum_{l=1}^L \left(\eta_l^2 \left(\frac{\beta_l}{1-\beta_l} \right)^2 \gamma^2 \frac{1-\beta_l}{1+\beta_l} \right) \sigma_l^2 + \sum_{l=1}^L \frac{\gamma \eta_l^2}{2} \sigma_l^2 \\
& \quad + \sum_{l=1}^L \left(-\eta_l + \frac{\eta_l}{2\rho_0} + \frac{\gamma \eta_l^2}{2} \right) \mathbb{E} \|\nabla_l \ell(\theta^t)\|^2 + 2\rho_0 \left(\sum_{l=1}^L \eta_l \right) \sum_{l=1}^L \left(\eta_l^2 \left(\frac{\beta_l}{1-\beta_l} \right)^2 \gamma^2 (1-\beta_l^{t-1})^2 \mathbb{E} \left[\|\nabla_l \ell(\theta^t)\|^2 \right] \right) \\
& \quad + 2\rho_0 \left(\sum_{l=1}^L \eta_l \right) \sum_{l=1}^L \left(\eta_l^2 \left(\frac{\beta_l}{1-\beta_l} \right)^2 \gamma^2 (1-\beta_l^{t-1})^2 \mathbb{E} \left[\left\| \frac{1-\beta_l}{1-\beta_l^{t-1}} \sum_{i=1}^{t-1} \beta_l^{t-1-i} \nabla_l \ell(\theta^i) - \nabla_l \ell(\theta^t) \right\|^2 \right] \right)
\end{aligned}$$

Now the last term above can be replaced since

$$\begin{aligned}
\mathbb{E} \left[\left\| \frac{1-\beta_l}{1-\beta_l^t} \sum_{i=1}^t \beta_l^{t-i} \nabla_l \ell(\theta^i) - \nabla_l \ell(\theta^t) \right\|^2 \right] & = \mathbb{E} \left[\left\| \frac{\beta_l(1-\beta_l)}{1-\beta_l^t} \sum_{i=1}^{t-1} \beta_l^{t-1-i} \nabla_l \ell(\theta^i) - \frac{1-\beta_l^{t-1}}{1-\beta_l^t} \beta_l \nabla_l \ell(\theta^t) \right\|^2 \right] \\
& = \beta_l^2 \left(\frac{1-\beta_l^{t-1}}{1-\beta_l^t} \right)^2 \mathbb{E} \left[\left\| \frac{1-\beta_l}{1-\beta_l^{t-1}} \sum_{i=1}^{t-1} \beta_l^{t-1-i} \nabla_l \ell(\theta^i) - \nabla_l \ell(\theta^t) \right\|^2 \right]
\end{aligned}$$

□

Now we return to the proof of Theorem 2.1.

Proof. [Proof of Theorem 2.1] By Proposition A.1 and Lemma A.2, we have

$$\begin{aligned}
& \mathbb{E} [\ell (z^{t+1})] \\
& \leq \mathbb{E} [\ell (z^t)] + \rho_0 \left(\sum_{l=1}^L \eta_l \right) \sum_{l=1}^L \left(\eta_l^2 \left(\frac{\beta_l}{1-\beta_l} \right)^2 \gamma^2 \frac{1-\beta_l}{1+\beta_l} \right) \sigma_l^2 + \sum_{l=1}^L \frac{\gamma \eta_l^2}{2} \sigma_l^2 \\
& \quad + \sum_{l=1}^L \left(-\eta_l + \frac{\eta_l}{2\rho_0} + \frac{\gamma \eta_l^2}{2} \right) \mathbb{E} \|\nabla_l \ell(\theta^t)\|^2 + 2\rho_0 \left(\sum_{l=1}^L \eta_l \right) \sum_{l=1}^L \left(\eta_l^2 \left(\frac{\beta_l}{1-\beta_l} \right)^2 \gamma^2 (1-\beta_l^{t-1})^2 \mathbb{E} \left[\|\nabla_l \ell(\theta^t)\|^2 \right] \right) \\
& \quad + 2\rho_0 \left(\sum_{l=1}^L \eta_l \right) \sum_{l=1}^L \left(\eta_l^2 \gamma^2 \left(\frac{1-\beta_l^t}{1-\beta_l} \right)^2 \sum_{i=1}^{t-1} a_{l,t,i} \mathbb{E} \left[\|\theta^{i+1} - \theta^i\|^2 \right] \right)
\end{aligned} \tag{A.7}$$

Now define the potential function:

$$\phi^t = \ell (z^t) - \ell^* + \sum_{i=1}^{t-1} \sum_{l=1}^L c_{l,i} \|\theta_l^{t+1-i} - \theta_l^{t-i}\|^2 \tag{A.8}$$

where $c_{l,i}$ are constants to be determined.

From (A.7) we get

$$\begin{aligned}
& \mathbb{E} [\phi^{t+1}] - \mathbb{E} [\phi^t] \\
& \leq \rho_0 \left(\sum_{l=1}^L \eta_l \right) \sum_{l=1}^L \left(\eta_l^2 \left(\frac{\beta_l}{1-\beta_l} \right)^2 \gamma^2 \frac{1-\beta_l}{1+\beta_l} \right) \sigma_l^2 + \sum_{l=1}^L \frac{\gamma \eta_l^2}{2} \sigma_l^2 \\
& \quad + \sum_{l=1}^L \left(-\eta_l + \frac{\eta_l}{2\rho_0} + \frac{\gamma \eta_l^2}{2} \right) \mathbb{E} \|\nabla_l \ell(\theta^t)\|^2 + 2\rho_0 \left(\sum_{l=1}^L \eta_l \right) \sum_{l=1}^L \left(\eta_l^2 \left(\frac{\beta_l}{1-\beta_l} \right)^2 \gamma^2 (1-\beta_l^{t-1})^2 \mathbb{E} \left[\|\nabla_l \ell(\theta^t)\|^2 \right] \right) \\
& \quad + 2\rho_0 \left(\sum_{l=1}^L \eta_l \right) \sum_{l=1}^L \left(\eta_l^2 \gamma^2 \left(\frac{1-\beta_l^t}{1-\beta_l} \right)^2 \sum_{i=1}^{t-1} a_{l,t,i} \mathbb{E} \left[\|\theta^{i+1} - \theta^i\|^2 \right] \right) \\
& \quad + \sum_{l=1}^L c_{l,1} \mathbb{E} \|\theta_l^{t+1} - \theta_l^t\|^2 + \sum_{i=1}^{t-1} \sum_{l=1}^L (c_{l,i+1} - c_{l,i}) \mathbb{E} \left[\|\theta_l^{t+1-i} - \theta_l^{t-i}\|^2 \right]
\end{aligned} \tag{A.9}$$

For the term $\sum_{l=1}^L c_{l,1} \mathbb{E} \|\theta_l^{t+1} - \theta_l^t\|^2$, we can bound it by (denote $\nabla_l^t = \nabla_{\theta_l} \ell(\theta^t)$)

$$\begin{aligned}
& \sum_{l=1}^L c_{l,1} \mathbb{E} \|\theta_l^{t+1} - \theta_l^t\|^2 = \sum_{l=1}^L c_{l,1} \eta_l^2 \mathbb{E} \left[\|m_l^t\|^2 \right] \\
& \leq 2 \sum_{l=1}^L c_{l,1} \mathbb{E} \left[\left\| m_l^t - (1 - \beta_l) \sum_{i=1}^t c_{l,1} \beta_l^{t-i} \nabla_l^i \right\|^2 \right] + 2 \sum_{l=1}^L \mathbb{E} \left[\left\| (1 - \beta_l) \sum_{i=1}^t \beta_l^{t-i} \nabla_l^i \right\|^2 \right] \\
& \leq 2 \sum_{l=1}^L c_{l,1} \frac{1 - \beta_l}{1 + \beta_l} \sigma_l^2 + 2 \sum_{l=1}^L c_{l,1} \mathbb{E} \left[\left\| (1 - \beta_l) \sum_{i=1}^t \beta_l^{t-i} \nabla_l^i \right\|^2 \right] \\
& \leq \sum_{l=1}^L c_{l,1} \eta_l^2 \left(2 \frac{1 - \beta_l}{1 + \beta_l} \sigma_l^2 + 4 \mathbb{E} \left[\|\nabla_l^t\|^2 \right] (1 - \beta_l^t)^2 \right) + 4 \sum_{l=1}^L c_{l,1} (1 - \beta_l^t)^2 \eta_l^2 \mathbb{E} \left[\left\| \frac{1 - \beta_l}{1 - \beta_l^t} \sum_{i=1}^t \beta_l^{t-i} \nabla_l^i - \nabla_l^t \right\|^2 \right] \\
& \leq \sum_{l=1}^L c_{l,1} \eta_l^2 \left(2 \frac{1 - \beta_l}{1 + \beta_l} \sigma_l^2 + 4 \mathbb{E} \left[\|\nabla_l^t\|^2 \right] \right) + 4 \sum_{l=1}^L c_{l,1} (1 - \beta_l^t)^2 \eta_l^2 \sum_{i=1}^{t-1} a_{l,t,i} \mathbb{E} \left[\|\theta^{i+1} - \theta^i\|^2 \right]
\end{aligned} \tag{A.10}$$

where for the last three inequalities we use (A.1) and

$$\mathbb{E} \left[\left\| \frac{1 - \beta_l}{1 - \beta_l^t} \sum_{i=1}^t \beta_l^{t-i} \nabla_l^i \right\|^2 \right] \leq 2 \mathbb{E} \left[\|\nabla_l^t\|^2 \right] + 2 \mathbb{E} \left[\left\| \frac{1 - \beta_l}{1 - \beta_l^t} \sum_{i=1}^t \beta_l^{t-i} \nabla_l^i - \nabla_l^t \right\|^2 \right],$$

and (A.2), respectively.

Now plugging this back to (A.9) we get:

$$\begin{aligned}
& \mathbb{E} [\phi^{t+1}] - \mathbb{E} [\phi^t] \\
& \leq \rho_0 s \sum_{l=1}^L \left(\eta_l^2 \left(\frac{\beta_l}{1 - \beta_l} \right)^2 \gamma^2 \frac{1 - \beta_l}{1 + \beta_l} \right) \sigma_l^2 + \sum_{l=1}^L \frac{\gamma \eta_l^2}{2} \sigma_l^2 + \sum_{l=1}^L 2 c_{l,1} \eta_l^2 \frac{1 - \beta_l}{1 + \beta_l} \sigma_l^2 \\
& \quad + \sum_{l=1}^L \left(-\eta_l + \frac{\eta_l}{2\rho_0} + \frac{\gamma \eta_l^2}{2} + 4 c_{l,1} \eta_l^2 \right) \mathbb{E} \|\nabla_l^t\|^2 + 2\rho_0 \left(\sum_{l=1}^L \eta_l \right) \sum_{l=1}^L \left(\eta_l^2 \left(\frac{\beta_l}{1 - \beta_l} \right)^2 \gamma^2 (1 - \beta_l^{t-1})^2 \mathbb{E} \left[\|\nabla_l^t\|^2 \right] \right) \\
& \quad + 4 \sum_{i=1}^{t-1} \sum_{l=1}^L c_{l,1} (1 - \beta_l^t)^2 \eta_l^2 a_{l,t,i} \mathbb{E} \left[\|\theta^{i+1} - \theta^i\|^2 \right] \\
& \quad + 2\rho_0 s \sum_{i=1}^{t-1} \sum_{l=1}^L \left(\eta_l^2 \gamma^2 \left(\frac{1 - \beta_l^t}{1 - \beta_l} \right)^2 a_{l,t,i} \mathbb{E} \left[\|\theta^{i+1} - \theta^i\|^2 \right] \right) \\
& \quad + \sum_{i=1}^{t-1} \sum_{l=1}^L (c_{l,i+1} - c_{l,i}) \mathbb{E} \left[\|\theta_l^{t+1-i} - \theta_l^{t-i}\|^2 \right]
\end{aligned} \tag{A.11}$$

where we denote $s := \sum_{l=1}^L \eta_l$.

To make the last three lines of above non-positive, we could take

$$c_{l,i+1} \leq c_{l,i} - \left(4 c_{l,1} (1 - \beta_l^t)^2 \eta_l^2 + 2\rho_0 s \eta_l^2 \gamma^2 \left(\frac{1 - \beta_l^t}{1 - \beta_l} \right)^2 \right) a_{l,t,t-i}$$

for all $l = 1, \dots, L$.

We can take (since $1 - \beta_l^t < 1$)

$$c_{l,i+1} = c_{l,i} - \left(4c_{l,1}\eta_l^2 + 2\rho_0 s \eta_l^2 \gamma^2 \left(\frac{1}{1-\beta_l} \right)^2 \right) \gamma^2 \beta_l^i \left(i + \frac{\beta_l}{1-\beta_l} \right)$$

also we can take $c_{l,1}$ such that

$$\begin{aligned} c_{l,1} &= \sum_{i=1}^{\infty} \left(4c_{l,1}\eta_l^2 + 2\rho_0 s \eta_l^2 \gamma^2 \left(\frac{1}{1-\beta_l} \right)^2 \right) \gamma^2 \beta_l^i \left(i + \frac{\beta_l}{1-\beta_l} \right) \\ &= \left(4c_{l,1}\eta_l^2 + 2\rho_0 s \eta_l^2 \gamma^2 \left(\frac{1}{1-\beta_l} \right)^2 \right) \gamma^2 \left(\sum_{i=1}^{\infty} i \beta_l^i + \frac{\beta_l}{1-\beta_l} \sum_{i=1}^{\infty} \beta_l^i \right) \\ &= \left(4c_{l,1}\eta_l^2 + 2\rho_0 s \eta_l^2 \gamma^2 \left(\frac{1}{1-\beta_l} \right)^2 \right) \frac{\gamma^2 \beta_l (1 + \beta_l)}{(1-\beta_l)^2} \end{aligned}$$

i.e.

$$c_{l,1} = \frac{2\rho_0 s \eta_l^2 \gamma^4 \beta_l \frac{1+\beta_l}{(1-\beta_l)^4}}{1 - 4\eta_l^2 \frac{\gamma^2 \beta_l (1+\beta_l)}{(1-\beta_l)^2}}. \quad (\text{A.12})$$

Note that we can give an upper bound for $c_{l,1}$ by requiring the denominator $\geq 1/2$, i.e.

$$\eta_l \leq \frac{1 - \beta_l}{\gamma \sqrt{8\beta_l(1 + \beta_l)}}, \quad (\text{A.13})$$

consequently

$$c_{l,1} \leq 4\rho_0 s \eta_l^2 \gamma^4 \beta_l \frac{1 + \beta_l}{(1 - \beta_l)^4}. \quad (\text{A.14})$$

Now we have (since the last three terms of (A.11) sum to negative)

$$\begin{aligned} &\mathbb{E} [\phi^{t+1}] - \mathbb{E} [\phi^t] \\ &\leq \rho_0 s \sum_{l=1}^L \left(\eta_l^2 \left(\frac{\beta_l}{1-\beta_l} \right)^2 \gamma^2 \frac{1-\beta_l}{1+\beta_l} \right) \sigma_l^2 + \sum_{l=1}^L \frac{\gamma \eta_l^2}{2} \sigma_l^2 + \sum_{l=1}^L 2c_{l,1} \eta_l^2 \frac{1-\beta_l}{1+\beta_l} \sigma_l^2 \\ &\quad + \sum_{l=1}^L \left(-\eta_l + \frac{\eta_l}{2\rho_0} + \frac{\gamma \eta_l^2}{2} + 4c_{l,1} \eta_l^2 + 2\rho_0 s \eta_l^2 \left(\frac{\beta_l}{1-\beta_l} \right)^2 \gamma^2 (1 - \beta_l^{t-1})^2 \right) \mathbb{E} \|\nabla_l^t\|^2 \end{aligned} \quad (\text{A.15})$$

Now take $\rho_0 = 2$, and take η_l such that

$$-\frac{3}{4}\eta_l + \frac{\gamma \eta_l^2}{2} + 4c_{l,1} \eta_l^2 + 4s \eta_l^2 \left(\frac{\beta_l}{1-\beta_l} \right)^2 \gamma^2 (1 - \beta_l^{t-1})^2 \leq -\frac{\eta_l}{2}, \quad (\text{A.16})$$

the coefficient of $\mathbb{E} \|\nabla_l^t\|^2$ can be greatly simplified. Note that we can guarantee (A.16) if

$$\eta_l \leq \min \left\{ \frac{1}{8\gamma}, \frac{1}{8\gamma L} \left(\frac{1-\beta_l}{\beta_l} \right)^2, \frac{1-\beta_l}{4\gamma} \sqrt[3]{\frac{1-\beta_l}{L\beta_l(1+\beta_l)}} \right\} \quad (\text{A.17})$$

for all $l = 1, 2, \dots, L$. Here each term in the right hand side of (A.17) is bounding each term on the left hand side of (A.16).

We get

$$\begin{aligned} \sum_{l=1}^L \frac{\eta_l}{2} \mathbb{E} \|\nabla_l^t\|^2 &\leq \mathbb{E} [\phi^t] - \mathbb{E} [\phi^{t+1}] \\ + 2s \sum_{l=1}^L \left(\eta_l^2 \left(\frac{\beta_l}{1-\beta_l} \right)^2 \gamma^2 \frac{1-\beta_l}{1+\beta_l} \right) \sigma_l^2 &+ \sum_{l=1}^L \frac{\gamma \eta_l^2}{2} \sigma_l^2 + \sum_{l=1}^L 2c_{l,1} \eta_l^2 \frac{1-\beta_l}{1+\beta_l} \sigma_l^2. \end{aligned} \quad (\text{A.18})$$

Note that we have defined $s := \sum_{l=1}^L \eta_l$. We can upper bound it by $s \leq L/\sqrt{\gamma T}$ if we assume $\eta_l \leq 1/\sqrt{\gamma T}$. Combining (A.13) and (A.17) we get:

$$\eta_l \leq \min \left\{ \frac{1}{8\gamma}, \frac{1}{8\gamma L} \left(\frac{1-\beta_l}{\beta_l} \right)^2, \frac{1-\beta_l}{\gamma \sqrt{8\beta_l(1+\beta_l)}}, \frac{1-\beta_l}{4\gamma} \sqrt[3]{\frac{1-\beta_l}{L\beta_l(1+\beta_l)}}, \frac{1}{\sqrt{\gamma T}} \right\}, \quad (\text{A.19})$$

which is satisfied if (since $\beta_l(1+\beta_l) \leq 2$)

$$\eta_l = \min \left\{ \frac{1}{8\gamma}, \frac{1}{8\gamma L} \left(\frac{1-\beta_l}{\beta_l} \right)^2, \frac{1-\beta_l}{4\gamma}, \frac{1-\beta_l}{4\gamma} \sqrt[3]{\frac{1-\beta_l}{2L}}, \frac{1}{\sqrt{\gamma T}} \right\}. \quad (\text{A.20})$$

By taking the product of two of the terms in the RHS of the above relation, we have the following upper bound on η_l^2 :

$$\eta_l^2 \leq \frac{1}{8\gamma L} \left(\frac{1-\beta_l}{\beta_l} \right)^2 \frac{1}{\sqrt{\gamma T}}. \quad (\text{A.21})$$

Plugging (A.21) and (A.14) into (A.18), we obtain:

$$\begin{aligned} \sum_{l=1}^L \eta_l \mathbb{E} \|\nabla_l^t\|^2 &\leq 2(\mathbb{E} [\phi^t] - \mathbb{E} [\phi^{t+1}]) \\ &+ \sum_{l=1}^L \left(\frac{1-\beta_l}{1+\beta_l} \frac{1}{4\gamma T} + \frac{1}{2T} + \frac{1-\beta_l}{\beta_l^3} \frac{\sqrt{\gamma}}{4L^2 T^{3/2}} \right) \sigma_l^2. \end{aligned} \quad (\text{A.22})$$

Now since $\beta_l \leq 1 - \delta$, we have that η_l is lower bounded

$$\begin{aligned} \eta_l &= \min \left\{ \frac{1}{8\gamma}, \frac{1}{8\gamma L} \left(\frac{1-\beta_l}{\beta_l} \right)^2, \frac{1-\beta_l}{4\gamma}, \frac{1-\beta_l}{4\gamma} \sqrt[3]{\frac{1-\beta_l}{2L}} \right\} \\ &\geq \min \left\{ \frac{1}{8\gamma}, \frac{\delta^2}{8\gamma L}, \frac{\delta}{4\gamma}, \frac{\delta}{4\gamma} \sqrt[3]{\frac{\delta}{2L}}, \frac{1}{\sqrt{\gamma T}} \right\} =: \eta \end{aligned} \quad (\text{A.23})$$

we obtain:

$$\begin{aligned} \sum_{l=1}^L \mathbb{E} \|\nabla_l^t\|^2 &\leq \frac{2(\mathbb{E} [\phi^t] - \mathbb{E} [\phi^{t+1}])}{\eta} \\ &+ \frac{1}{\eta} \sum_{l=1}^L \left(\frac{1-\beta_l}{1+\beta_l} \frac{1}{4\gamma T} + \frac{1}{2T} + \frac{1-\beta_l}{\beta_l^3} \frac{\sqrt{\gamma}}{4L^2 T^{3/2}} \right) \sigma_l^2. \end{aligned} \quad (\text{A.24})$$

Now by telescoping sum of (A.22) for $t = 1, \dots, T$, also notice that $1/\eta = \Theta(\sqrt{\gamma T} L \gamma / \delta^2)$ as T grows, we get our final result of

$$\frac{1}{T} \sum_{t=1}^T \sum_{l=1}^L \mathbb{E} \|\nabla_l^t\|^2 \leq \frac{2L\gamma^{3/2} \mathbb{E} \Delta_1}{\delta^2 \sqrt{T}} + \sum_{l=1}^L \left(\frac{1 - \beta_l L \sqrt{\gamma}}{1 + \beta_l 4\sqrt{T}} + \frac{L\gamma^{3/2}}{2\sqrt{T}} + \frac{1 - \beta_l \gamma^2}{\beta_l^3 4LT} \right) \frac{\sigma_l^2}{\delta^2}. \quad (\text{A.25})$$

This completes the proof. □